

# Fabrication and spectroscopy of Cs vapor cells with buffer gas for miniature atomic clock

D. Miletic<sup>1</sup>, C. Affolderbach<sup>1</sup>, E. Breschi<sup>1</sup>, C. Schori<sup>1</sup>, G. Mileti<sup>1</sup>, M. Hasegawa<sup>2</sup>, R. Chutani<sup>2</sup>, P. Dziuban<sup>2</sup>, R. Boudot<sup>2</sup>, V. Giordano<sup>2</sup>, C. Gorecki<sup>2</sup>

<sup>(1)</sup> *Laboratoire Temps-Fréquence, Université de Neuchâtel, Neuchâtel, Switzerland*

<sup>(2)</sup> *FEMTO-ST, CNRS and UFC, Besançon, France*

The Coherent Population Trapping (CPT) phenomenon can be observed in alkali atoms D-lines by coupling two hyperfine ground-state Zeeman sub-levels to a common excited state using two coherent electromagnetic fields in a so-called  $\Lambda$ -scheme [1]. When the Raman resonance condition is satisfied, the atoms are trapped in a coherent superposition of the ground-states (the dark state) where, in ideal case, they do not absorb incident photons anymore. The interest of studying CPT-based atomic clocks is related to the fact that the dark line spectroscopy does not require microwave cavity allowing a strong miniaturization of the device [2].

We report on the realization and spectroscopic characterization of micro-fabricated caesium (Cs) vapour cells for applications in miniature atomic frequency standards. The mini-cell contains Cs atomic vapor and is filled with a pressure of buffer gas (Ne or Ar). The main effects of the buffer gas are to prevent the Cs ground-state spin relaxation by strongly decreasing the rate of collisions between the Cs atoms and the cell glass walls and by reducing time-of-flight broadening and by inducing Dicke narrowing [3]. With this technique the resonance line-width is strongly reduced with respect to the one that can be observed by preparing the resonance in a simple, buffer-gas free cell of the same dimensions.

In a first section of this communication, we present the experimental setup with emphasis on the fabrication process of the mini-cells. In a second section we study the influence of some critical experimental parameters such as laser power and temperature on the dark resonance characteristics (linewidth, amplitude, etc.). In a last section, preliminary short-term stability performances of a CPT clock based on such microcells are reported. A short term stability of  $5 \times 10^{-10}$  at 1s, in correct agreement with signal-to-noise ratio measurements is obtained.

## Experimental setup

The block diagram of the experimental set-up is represented in fig. 1. The dark resonance is prepared by using a DFB laser emitting at 894.6 nm i.e., resonant with the Cs D1-line. The choice of the D1-line is expected to reach a resonance with higher contrast and narrower linewidth compared to the excitation of the D2-line [4]. The laser frequency is locked on Doppler-broadened absorption line by modulating the laser DC current at 50 kHz and demodulating the photodiode signal with a Lock-In amplifier. The DFB presents a line-width lower than 15 MHz, a relative intensity noise (RIN) at 500Hz of  $8 \times 10^{-14} \text{ Hz}^{-1}$ , a frequency noise of about  $9 \text{ kHz} / \text{Hz}^{1/2}$  [5] and a laser beam diameter of about 2 mm. Two phase-coherent electromagnetic fields, separated by  $2\nu \sim 9.2 \text{ GHz}$ , are generated by modulating the optical beam at  $\nu \sim 4.6 \text{ GHz}$  (the two first order sidebands are used for to create the  $\Lambda$ -scheme) using a fibre-coupled Electro-Optical Modulator (EOM). At the output of the EOM, the collimated beam is attenuated with a variable neutral density filter, circularly polarized and finally sent through the mini-cell. In the clock physics package, the cell is carefully temperature controlled, surrounded by a solenoid generating a static magnetic field parallel to the light propagation vector to separate Zeeman sublevels. The ensemble is surrounded by  $2 \mu\text{m}$ -metal magnetic shields. The mini-cell temperature can be stabilized at the mK level in the temperature range  $45^\circ\text{C}$ - $90^\circ\text{C}$  temperature range. The 4.6GHz is generated by a commercial frequency synthesizer, referenced to a 10 MHz quartz local oscillator.

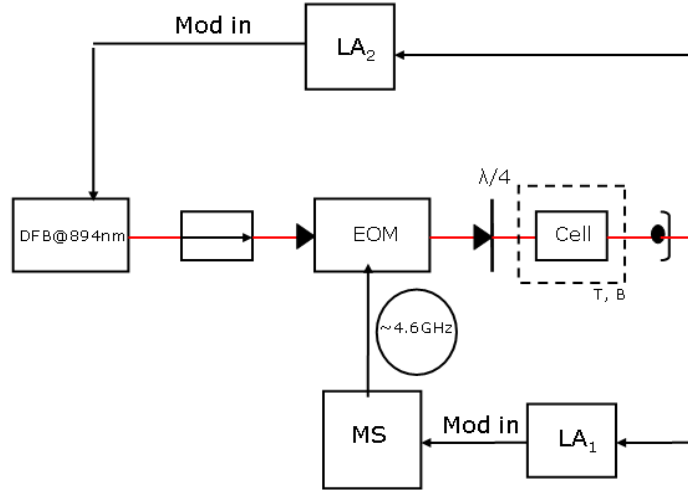


Fig. 1: Block diagram of the experimental setup. MS: microwave synthesizer. LA: lock-in amplifier.

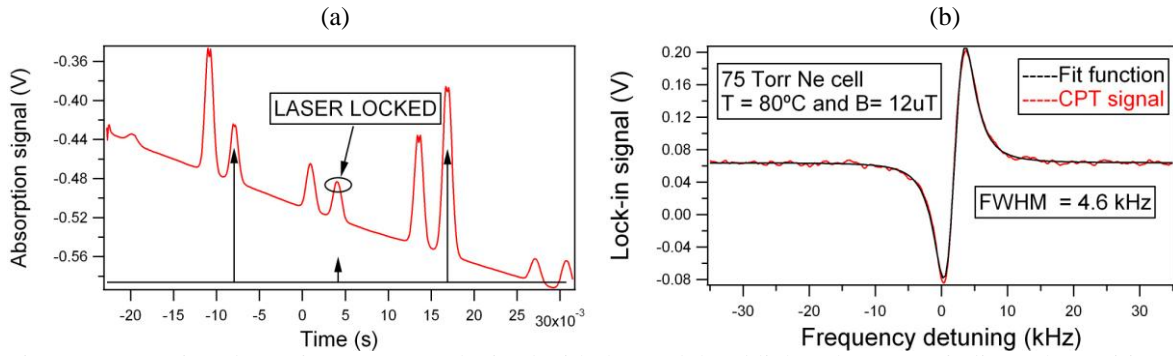


Fig.2 (a) Saturation absorption spectrum obtained with the modulated light. The arrows indicate the position of the carrier and 1<sup>st</sup>-order side-bands of the laser spectral distribution in clock configuration. (b) The lock-in in-phase signal due to the CPT-effect prepared in Cs atoms contained in a mini-cell with 75 torr of Ne at 80°C.

We create CPT resonances by driving optical transitions to the  $F=3$  excited state. The typical configuration of the excitation scheme is shown in Fig. 2(a): the red line is the saturated absorption spectrum recorded by spanning the frequency of the modulated laser through the D1-line in an evacuated reference cell, and the dark arrows show the detuning of the carrier and the first-order side-bands when the clock resonance is excited. To increase the signal-to-noise ratio the frequency  $\nu$  is modulated at 556 Hz and the reference resonance is detected with a lock-in amplifier. An example of CPT resonance is reported in Fig 2(b). The line-width of the resonance is about 9.2 kHz (the factor two with respect to the x-axis of Fig. 2(b) comes from the modulation at  $\nu$  which is about half of the hyperfine splitting of the Cs ground-states).

### MEMS cell fabrication and activation

The MEMS Cs vapour cell consists of a glass/Si/glass structure containing two cavities as described in [6] and shown in Fig. 3. The dimensions of a single cell chip are (4 x 6) mm and 2.4 mm thick. The first cavity contains a Cs metallic dispenser while the second cavity is devoted to be the volume where the CPT interaction takes place. Both cavities are connected together through filtration channels. In a first step, a glass wafer is anodically bonded to the Si wafer in which both cavities are realized by deep reactive ion etching techniques. A Cs dispenser is then placed in the first cavity. In a second step the cell is completely sealed by anodically bonding a second glass wafer on the top surface of the Si wafer in a buffer gas atmosphere (Ne or Ar) at the desired pressure. After the complete sealing of the cell, the Cs dispenser is heated by a high-power 808 nm laser source in order to generate Cs vapour that migrates to the second cavity. The activation time is typically 1-6 minutes for a laser power of 1.25W. This technique is expected to allow to keep a stable atmosphere inside the cell because Cs vapour activation is done after anodic bonding processes requiring high temperatures (350°C).

After fabrication, preliminary linear absorption measurements are realized to confirm the presence of cesium and buffer gas inside the microfabricated cell. For this purpose, the optical beam of a single 852 nm DBR (Distributed Bragg Resonator) diode laser whose injection current is slowly ramp modulated is splitted into two directions and sent through the tested microcell and a macroscopic pure Cs reference cell. The transmitted optical power at the output of each cell is then monitored by a low noise photodiode. Figure 4(a) shows the optical linear absorption spectrum of Cs D2 transition obtained for a microcell filled with an expected Argon pressure of 50 torr for different temperatures compared to the spectrum obtained from the reference cell at a temperature of 21°C. The presence of buffer gas in the microcell is demonstrated by broadening and red shift of the optical absorption lines. In this example, employing data reported in the article from Bernabeu et al [7], the actual buffer gas pressure in the microcell is measured to be about 47.8 torr. Correct reproducibility of the actual buffer gas pressure of microcells coming from the same wafer has been observed. Thermal aging behaviour has also been investigated to verify that the internal cell atmosphere remains constant along time. The lifetime of the cell is estimated by the so-called  $Q_{10}=2$  method assuming that the rate of aging increases by a factor of 2 for every 10°C increase in temperature. Figure 4(b) shows the evolution versus time of the amplitude of the  $6S_{1/2} F=4 \rightarrow 6P_{3/2}$  transition in a microcell filled with 10 torr of Argon and heated at a temperature of 75°C. Despite the slight fluctuations attributed to technical noise and the variations in the laboratory environment, it is clearly observed that the peak height does not change significantly for a time period higher than 1 month. Recently, for 55 days-long thermal test performed at 100°C during which absorption lines have been recorded periodically, we are confident that the atmosphere of a microcell kept about unchanged. The lifetime of this cell is then expected to be at least 220 days at 80°C. Nevertheless, this measurement is currently still in progress to validate strongly the fact that the anodic bonding strength is sufficient to maintain a stable atmosphere inside the cell without degradation along long integration time.

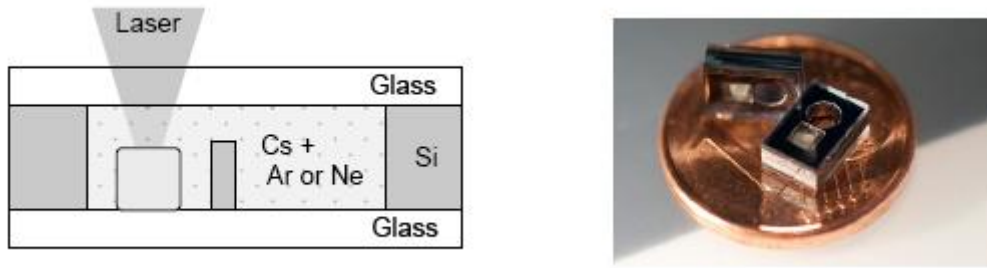


Fig. 3: Schematic of the structure of the microcell and photograph of the microcell.

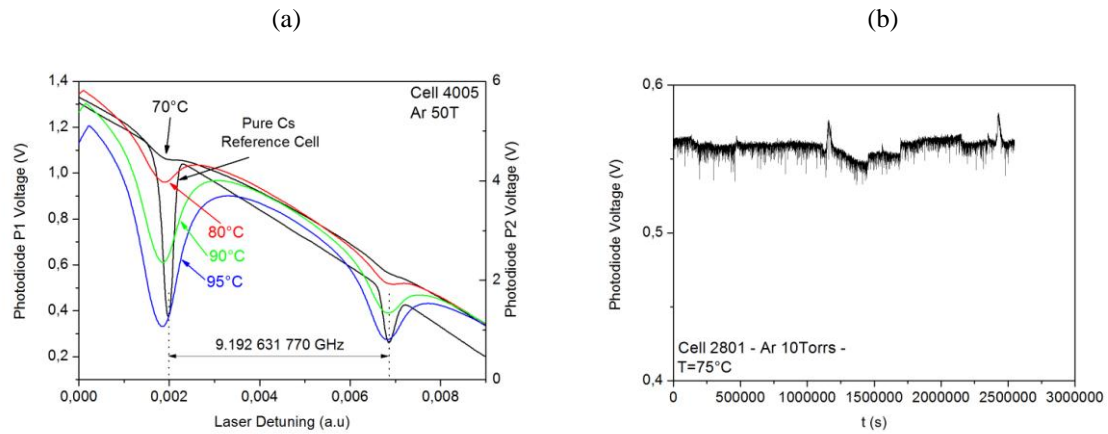


Figure 4: (a) Optical absorption lines (Cs D2 line) obtained in a micro-fabricated cell filled with an expected Argon pressure of 50 torr (measured to be 47.8 torr after sealing of the cell) at various temperatures compared to lines obtained in a centimetre-scale pure Cs reference cell at 21°C, (b) Evolution of the absorption line height for a microcell filled with a 10 torr Ar pressure heated at 75°C versus time.

## Coherent population trapping spectroscopy

We study the dark resonance parameters (amplitude, linewidth and resonance frequency) in a 75 torr Ne microcell versus the laser intensity [8] for different cell temperatures [9] in the range 45°C-90°C. Here we briefly summarize the main results. Further work is in progress in order to fully characterize the resonance.

In Fig. 5(a) and (b) the resonance amplitude and linewidth are represented as a function of the total laser power for a cell temperature of 80°C. Both resonance parameters show a linear dependence with respect to the laser power. This indicates that the resonance line-width is mainly determined by the power broadening effect, but the laser power is still below the saturation limit. In Fig.6 (a) we present a series of measurements of the resonance frequency as a function of the laser power (the so-called light shift) for different values of the cell temperature. This study allows us to determine the temperature coefficient of the micro-fabricated cell with 75 torr Ne content. In fact the dependence of the observed light shift is linear, and therefore we can easily extrapolate the value of the frequency to zero laser power. This simple procedure allows us to isolate the effect of the cell temperature.

The results are shown in Fig. 6(b) where the points are the experimental results while the line is the parabolic fit of this set of measurements. The data indicates that the temperature shift presents a quadratic dependence, i.e., the first order dependence is suppressed. We measure an inversion temperature  $T_{\text{inv}} \approx 73^\circ\text{C}$ . Note that the cancellation of the linear temperature shift at fixed working temperature is normally achieved by filling the cell with an appropriate mixture of different buffer gases, induce the linear temperature shifts of opposite signs cancel out [10]. Based on our experimental results, it is shown that it is possible to reach a quadratic temperature shift regime in a Cs microfabricated cell, using only pure Ne as a buffer gas, at appropriately chosen cell temperature and buffer gas pressure (here approximately 73°C and 75 torr, respectively). Further experiments are in progress in order to confirm and obtain with better resolution this important result.

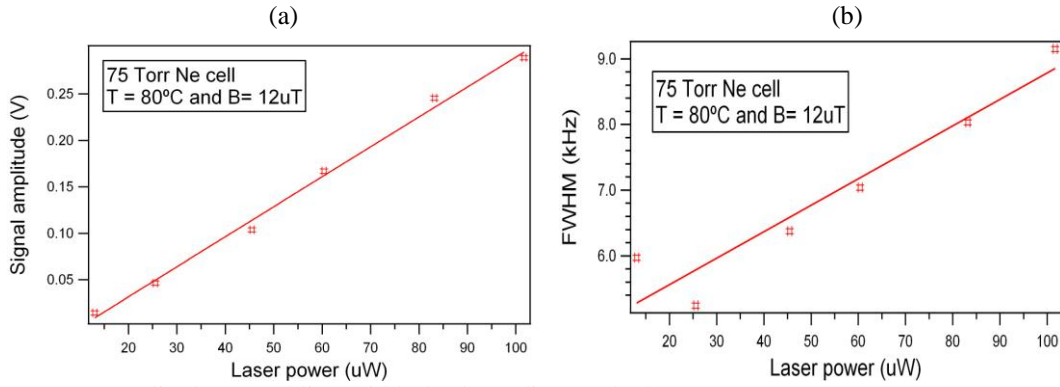


Fig. 5: Resonance amplitude (a) and line-width (b) depending on the laser power.

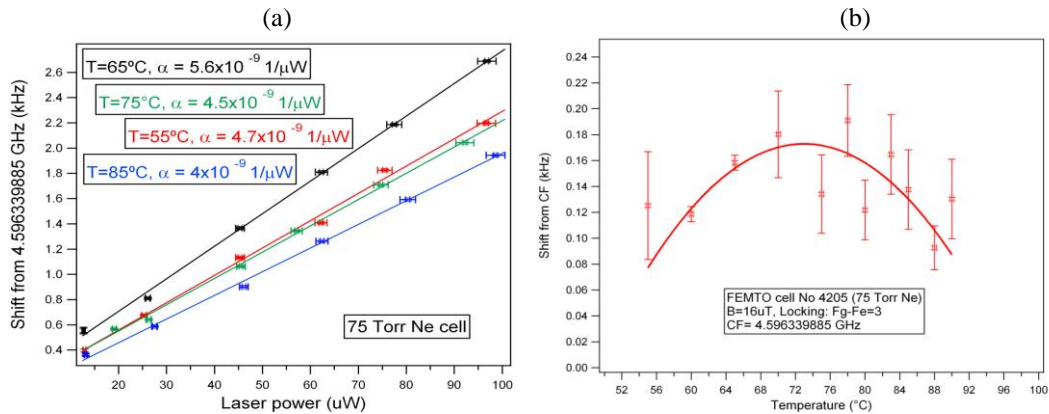


Fig. 6: (a) Resonance frequency shift as a function of the total laser power (light shift) for different values of the cell temperature. (b) Resonance frequency shift extrapolated at zero laser power as a function of the cell temperature (temperature shift).

## Stability measurement

The clock short-term frequency stability, described by the Allan deviation ( $\sigma_y(\tau)$ ) can be estimated by the detection noise (noisePSD) and the resonance discriminator slope ( $D$ ), following the formula [11]:

$$\sigma_y(\tau) = \frac{\text{noisePSD}}{\sqrt{2}D\nu} \cdot \tau^{-1/2} \quad (1)$$

where  $\nu$  is the microwave modulation frequency (equal to 4.596 GHz, in our case).

The detection noise includes the noise contributions from the photo-detector circuit, the detection shot-noise, and the laser noise; while  $D$  depends on the reference resonance amplitude and line-width (see Fig. 2(b)).

After preliminary optimization of the relevant experimental parameters (for instance the laser power, the laser polarization and the cell temperature) to obtain a signal with high contrast and narrow line-width we measured the detection noise to calculate the expected value of the Allan deviation using (1). To measure the clock stability the 10 MHz output of the local quartz oscillator is compared to the signal delivered by a hydrogen maser, using a Picotime phase comparator. The results of preliminary short-term stability measurements are reported in Fig. 7. The points represent the Allan deviation values calculated from the experimental measurements while the line is the prediction based on the signal-to-noise ratio measurements. The clock has a short-term stability of  $5 \times 10^{-10} \tau^{-1/2}$  at 1s in good agreement with the value of  $4.3 \times 10^{-10} \tau^{-1/2}$  predicted from (1). Further studies will address how to further improve on the clock's short term stability, as well as the origin of the observed stability degradation at  $\tau \geq 100$ s (possible due to variations in the environmental temperature and laser intensity).

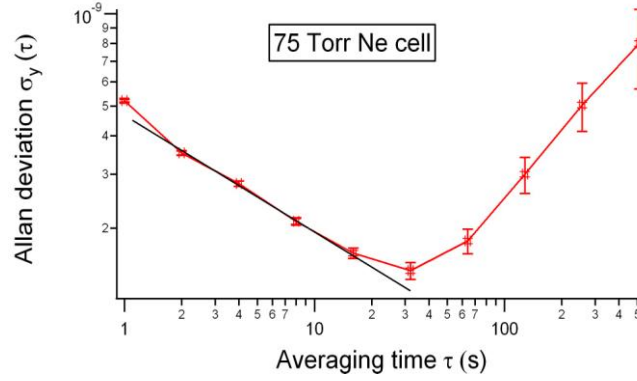


Fig.7: Short-term clock stability measurement.

## CONCLUSIONS

In this communication we discuss the fabrication and spectroscopic characterization of original micro-fabricated Cs cells filled with buffer gas in view of applications in miniature atomic clocks. The influence of several experimental parameters on CPT resonances in such micro cells is studied. We observed a quadratic temperature dependence of the clock frequency in a micro-fabricated cell filled with Cs and pure Ne buffer gas. This results in a low temperature coefficient around the inversion temperature, and relaxes the stability requirements on the cell temperature and should improve the clock's long term stability. The possibility to achieve such low temperature coefficient using a single type of buffer gas can noticeably simplify the technique of the cell production. Indeed, the control of the buffer-gas represents a difficult challenge in micro-fabricated cells production. Finally we report on preliminary short term clock stability measurements. A stability of  $5 \times 10^{-10} \tau^{-1/2}$  @ 1s is obtained. This value is in good agreement with the signal-to-noise stability prediction but remains to be improved.

## ACKNOWLEDGMENTS

We acknowledge financial support by the European Seventh Framework Programme FP7. This work was also supported by the Swiss National Science Foundation (project 200020-118062). We thank F. Gruet for the laser system mounting and characterisation and the following colleagues from LTF-UniNe for their contributions to the realisation of the hardware: P. Scherler, M. Durrenberger, J. Di Francesco and D. Varidel.

## REFERENCES

1. G. Alzetta, A. Gozzini, M. Moi, and G. Orriols, "An experimental method for the observation of R.F. transitions and laser beat resonances in oriented Na vapor," *Nuovo Cimento*, vol. B36, pp. 5–20, 1976.
2. J. Kitching, S. Knappe, L. Hollberg, "Miniature vapor-cell atomic-frequency references," *Appl. Phys. Lett.*, vol. 81, n. 3, pp. 553-556, 2002.
3. R. H. Dicke, "The effect of collisions upon the doppler width of spectral lines," *Phys. Rev. Lett.*, vol. 89, pp. 472–473, 1953. S. Brandt, A. Nagel, R. Wynands, D. Meschede, "Buffer-gas-induced linewidth reduction of coherent dark resonances to below 50 Hz", *Phys. Rev. A*, vol. 56, n. 2, pp. R1063 – 1066, 1997.
4. M. Stähler, R. Wynand, S. Knappe, J. Kitching, L. Hollberg, A. Taichenachev, and V. Yuding, "Coherent population trapping resonances in thermal 85Rb vapor: D1 versus D2 line excitation" *Opt. Lett.*, vol. 27, i. 16, pp. 1472-1474, 2002.
5. F. Gruet, D. Miletic, C. Affolderbach, G. Miletic, V. Vilokinen, P. Melanen, "Spectral characterization of aged and non-aged 894 nm DFB for their application in Cs atomic clocks", *Proc. of the International Symposium on Reliability of Optoelectronics for Space (ISROS)*, Cagliari (I), pp. 1-14, May 2009.
6. A. Douahi, L. Nieradko, J.C. Beugnot, J. Dziuban, H. Maillote, S. Guérandel, M. Moraja, C. Gorecki, and V. Giordano, "Vapour microcell for chip scale atomic frequency standard", *Electron. Lett.*, vol. 43, pp.279, 2007.
7. L. Nieradko et al., "New approach of fabrication and dispensing of micromachined cesium vapor cell", *J. Micro-Nanolithogr. MEMS MOEMS*, vol. 7, pp. 033013, 2008.
8. S. Knappe, J. Kitching, L. Hollberg, R. Wynands, "Temperature dependence of coherent population trapping resonances", *Appl. Phys. B*, vol. 74, pp. 217-22, 2002.
9. S. Knappe, R. Wynands, J. Kitching, H. G. Robinson, L. Hollberg, "Characterization of coherent population trapping resonances as atomic frequency references", *J. Opt. Soc. Am. B.*, vol. 18 n. 11 pp.1545-1553, 2001.
10. J. Vanier, R. Kunski, N. Cyr, J. Y. Savard and M. Têtu, "On hyperfine frequency shifts caused by buffer gases: Application to the optically pumped passive rubidium frequency standard", *J. Appl. Phys.*, vol. 43, pp. 5387-5391, 1982.
11. G. Miletic, P. Thomann, "Study of the S/N performance of passive atomic clocks using a laser pumped vapour" *Proceeding of EFTF*, pp. 271-276, 1995.